The Crystal Structures of Two Nitroprussides: Mn[Fe(CN)$_5$NO]·3H$_2$O and Cd[Fe(CN)$_5$NO]·3H$_2$O

D. F. MULLICA, D. B. TIPPIN and E. L. SAPPENFIELD

Department of Chemistry, Baylor University, Waco, TX 76798 (U.S.A.)

(Received November 21, 1989; revised March 28, 1990)

Abstract

The crystal structures of manganese(II) and cadmium(II) nitrosylpentacyanoferrate trihydrate have been determined from three dimensional, single-crystal X-ray diffraction data. These polynuclear cyanides crystallize in the monoclinic space group $P2_1/n$ (No. 14, C_{2h}^5) with four formula units per cell. The lattice constants are $a = 7.302(4)$, $b = 14.783(6)$, $c = 10.751(1)$ Å and $\beta = 91.47(2)°$ for manganese nitroprusside and $a = 7.425(2)$, $b = 14.963(2)$, $c = 10.848(3)$ Å and $\beta = 91.64(2)°$ for cadmium nitroprusside. $D_m = 1.86(1)$ Mg m^{-3}, $D_x = 1.864$ Mg m^{-3} and $D_m = 2.09(1)$ Mg m^{-3}, $D_x = 2.106$ Mg m^{-3}, respectively for manganese and cadmium nitroprusside. Final full-matrix least-squares refinement of 1881 unique reflections for Mn[Fe(CN)$_5$NO] and 1958 unique reflections for Cd[Fe(CN)$_5$NO] yielded $R = 0.023$ and 0.030, respectively. Both iron and divalent metal centers have distorted octahedral symmetries. The iron atom is coordinated by five cyanide ligands and one nitrosyl group, whereas the cation metal center is coordinated by five cyanide ligands and one water molecule. The metal atoms in both structures are linked by Fe–C≡N–M bridging (M = Mn or Cd). The two uncoordinated water molecules, O(2) and O(3), are hydrogen bonded to the coordinated water molecule, O(1), and occupy channels in the crystal lattice. Important mean bond lengths for manganese nitroprusside are: Mn–N = 2.226(19), Fe–C = 1.935(5) and C≡N = 1.140(2) Å. Other notable bond lengths include Mn–O(1) = 2.218(2), Fe–N = 1.659(2) and N=O = 1.135(2) Å as well as the contact distances O(1)–O(2) = 2.854(3) and O(1)–O(3) = 2.759(3) Å. Important mean bond distances for cadmium nitroprusside are Cd–N = 2.314(18), Fe–C = 1.942(6) and C≡N = 1.135(7) Å. Other notable bond and contact distances include Cd–O(1) = 2.335(2), Fe–N = 1.667(3), N=O = 1.125(3), O(1)–O(2) = 2.856(4) and O(1)–O(3) = 2.784(4) Å.

Introduction

For decades the ferricyanides have been known to uptake water, ammonia and other small molecules from the air. The hexacyanides have been the most widely studied of the ferricyanides and have been employed as molecular sieves, cation exchangers, electron scavengers and most recently as radionuclide sorbents [1, 2]. Within many hexacyanides, channels are formed by systematic [Fe(CN)$_6$]$^{3-}$ vacancies in the structural array, which give rise to pore sizes of *c.* 5.6 × 8.6 Å [3]. The extensive π-bridging and open channels throughout the lattice are primarily responsible for the unique properties of the ferricyanides. However, in the case of the nitrosylpentacyanides the cyanide complexes possess no vacancies and channels are the result of unbridged nitrosyl groups [4]. These channels are significantly smaller than their hexacyanide counterparts, offering greater selectivity in the separation of smaller molecules. Compared to the classical silica–alumina molecular sieves, the ferrocyanides allow a more flexible change in both the geometry and dimensions of their pores. Not only can the cation and anion metal cores be varied but also the types of monosubstituted ligands, e.g. NO for CN. Furthermore, many cyanometallates undergo a noticeable color change upon dehydration, which provides an easy check of this process.

Many transition metal hexacyanides have been shown to crystallize in the same face-centered cubic (f.c.c.) space group as Prussian blue, $Fm\bar{3}m$ [5, 6]. However, despite the similarities and possible uses of the nitroprussides, few single-crystal analyses have been cited in the literature. Studies of the titled nitroprussides were initiated due to interest in their semi-permeable membrane properties and their possible use as radionuclide sorbents in nuclear waste management.

Experimental

Commercially available analytical reagent grade Na$_2$Fe(CN)$_5$NO·2H$_2$O, MnCl$_2$ and CdCl$_2$ were used as starting materials. The 'slow-diffusion-tube' method was employed to synthesize the titled compounds [4]. The diffusion tube apparatuses were stored in the dark, and within two to three months, crystals large enough for single-crystal analysis were

0020-1693/90/$3.50

TABLE 1. Experimental amd statistical summaries of $Mn[Fe(CN)_5NO]\cdot 3H_2O$ and $Cd[Fe(CN)_5NO]\cdot 3H_2O$

	$Mn[Fe(CN)_5NO]\cdot 3H_2O$	$Cd[Fe(CN)_5NO]\cdot 3H_2O$
Space group	$P2_1/n$ (No. 14, C_{2h}^5)	$P2_1/n$ (No. 14, C_{2h}^5)
a (Å)	7.302(4)	7.425(2)
b (Å)	14.783(6)	14.963(2)
c (Å)	10.751(1)	10.848(3)
β (°)	91.47(2)	91.64(2)
V (Å^3)	1160.2	1204.7
D_m (Mg m^{-3})	1.86(1)	2.09(1)
D_x (Mg m^{-3})	1.864	2.106
M_r	324.92	328.26
Z	4	4
$F(000)$ (e$^-$)	644	736
μ (Mo K$\bar{\alpha}$) (mm^{-1})	2.32	2.97
$\Delta\theta$ (°)	1.5–25.0	1.5–25.0
$\Delta\omega$ (°) (ω–2θ scan)	1.20 + 0.35 tan θ	1.20 + 0.35 tan θ
R_{int}	0.016	0.025
R	0.023	0.030
R_w	0.030	0.038
Unique reflections ($>3\sigma(I)$)	1881	1958
g (e^{-2}) ($\times 10^{-7}$)	12.1(1)	2.0(1)
Shift/error ($\Delta\zeta_i/\sigma(\zeta_i)$) ($\times 10^{-4}$)		
maximum	6.53	3.90
average	0.40	0.40
Residual density (e$^-$ Å^{-3})		
maximum	0.56(3)	0.80(4)
minimum	−0.37(3)	−0.82(4)
Goodness of fit (Σ_2)	1.50	1.56

obtained. Using the flotation method (bromoform and 1-hexene), the densities of $Mn[Fe(CN)_5NO]\cdot 3H_2O$ and $Cd[Fe(CN)_5NO]\cdot 3H_2O$ were determined, see Table 1. Thermal dehydration of the title compounds was determined by employing a Perkin-Elmer TGS-1 thermobalance. The thermogravimetric analyses indicated three water molecules per formula unit for each newly harvested sample. Dehydration of both compounds appears to occur in a stepwise manner. In each, one water molecule is lost almost immediately upon standing, i.e. monodehydration ensues, followed by a gradual loss of the remaining water molecules as the temperature of the crystal is raised. This was evidenced by allowing crystals of both compounds to air dry for approximately two days after which elevated thermal analyses revealed losses of only two water molecules. Furthermore, air-drying caused the crystals of both compounds to become brittle, reducing them to a powder crystalline material when handled. For this reason, it was obvious that single crystals would have to be placed in glass capillaries with their mother liquor for X-ray analysis. Infrared spectroscopic analyses of pressed KBr/sample pellets were carried out on a Mattson Fourier Transform IR analyzer over the frequency range 4000 to 400 cm^{-1}; the results obtained from the absorption spectrum are presented in Table 2. In addition, biaxial symmetry for each system was confirmed by conoscopic examinations, which were performed by crystal rotation between two crossed polarizers on a Zeiss Photomicroscope II.

Single crystals of $Mn[Fe(CN)_5NO]\cdot 3H_2O$ and $Cd[Fe(CN)_5NO]\cdot 3H_2O$, selected on the basis of size and optical purity, were mounted on an Enraf-Nonius CAD-4F automated diffractometer equipped with a dense graphite monochromator, take-off angle equal to 5.8° (Mo K$\bar{\alpha}$ radiation, $\lambda_{mean} = 0.71073$ Å). The orientation matrices and single-crystal lattice parameters (final unit cell parameters at high θ angles, $>22°$) were obtained from the least-squares refinement of 25 randomly selected and accurately centered reflections. The lattice parameters and other pertinent experimental and statistical data are listed in Table 1. Data sets were then collected for each transition metal nitrosylpentacyanide over the range of $3.0° < 2\theta < 50.0°$ utilizing the ω–2θ scan technique at a varied scan rate (0.38–3.35° min^{-1}) which was determined by a fast prescan of 3.35° min^{-1}. All reflections having less than 75 counts above background during the fast prescan were assumed to be unobserved. In order to check the crystals and the reliability and stability of the electronic hardware, two reflections from each data set (Mn: $\bar{3}\,\bar{1}\,\bar{3}$ and $1\,\bar{2}\,2$; Cd: $3\,\bar{2}\,2$ and $3\,5\,\bar{1}$) were selected as standards and monitored every 2 h of exposure time. No significant variations (0.8 and

TABLE 2. Infrared frequencies for $Mn[Fe(CN)_5NO]\cdot 3H_2O$ and $Cd[Fe(CN)_5NO]\cdot 3H_2O$ [a]

Assignment	$Mn[Fe(CN)_5NO]\cdot 3H_2O$		$Cd[Fe(CN)_5NO]\cdot 3H_2O$ [b]	
	Wavenumber (cm^{-1})	Transmission (%)	Wavenumber (cm^{-1})	Transmission (%)
N=O (2ν)	3850w,br	49.9	3865	24.9
O–H (ν)	3656	23.7	3671	8.8
	3630sh	42.0	3636	15.7
	3597	36.7	3602	25.3
	3575sh	38.0	3584	15.9
O–H (ν) intermolecular H-bonding	3414br	22.9	3314	26.4
	3210sh,br	36.0	3232	23.0
C≡N (ν)	2195	8.5	2196	4.0
	2165sh	68.0	2180	0.9
N=O (ν)	1945	5.3	1952	0.4
H–O–H (δ)	1635sh	68.0	1650	44.3
	1619	22.6	1607	8.7
H–O–H (L)	760sh,br	38.0	740	34.0
Fe–NO (δ)	669	33.1	663	16.1
Fe–NO (ν)	654	40.7	653	33.8
Fe–CN (δ)	519	37.0	516	13.4
Fe–CN (ν)	442	9.6	440	0.9
	431	14.4	428	1.0

[a] br = broad, sh = shoulder, w = weak, L = libration. [b] All peaks were well pronounced.

0.6%, respectively) were observed in the intensities of the check reflections. Of the 2787 collected reflections (h: $-3 \rightarrow 8$; k: $-7 \rightarrow 17$; l: $-12 \rightarrow 12$) for $Mn[Fe(CN)_5NO]\cdot 3H_2O$ and of the 2503 collected reflections (h: $0 \rightarrow 8$; k: $0 \rightarrow 17$; l: $-12 \rightarrow 12$) for $Cd[Fe(CN)_5NO]\cdot 3H_2O$, 1881 and 1958 reflections fitted $I_{net} > 3\sigma(I)$, respectively. Lorentz, polarization and absorption corrections were applied to each data set. Systematic absences ($h0l$, $h + l = 2n + 1$ and $0k0$, $k = 2n + 1$) in each system were consistent with space group $P2_1/n$. Additional examination of the collected data sets using an N(Z) cumulative probability distribution test provide further evidence of a centrosymmetric system.

Crystallographic analyses of the reduced and averaged data employing MULTAN [7] revealed the initial locations of the transition metals and iron centers. Consequently, difference Fourier mapping of the residual electron density disclosed the locations of the remaining non-hydrogen atoms in both structures, including the positions of the oxygen atoms (water molecules). The model for both systems was refined by the full-matrix least-squares method [7]. After applying secondary extinction corrections (g) and several cycles of anisotropic refinements, residual factors were finalized, $R = \Sigma\Delta F/\Sigma|F_o|$ and $R_w = \Sigma\sqrt{w}\Delta F/\Sigma\sqrt{w}|F_o|$ where $\Delta F = ||F_o| - |F_c||$ and $w = \sigma^{-2}(|F_o|)$, see Table 1. The 'goodness-of-fit' values (Σ_2) and the values of abscission ($\Delta\zeta_i/\sigma(\zeta_i)$ where ζ_i are varied parameters) are also found in Table 1. Final electron density maps were truly featureless, revealing only random, fluctuating backgrounds with respective maximum peaks of 0.56 and 0.80 $e^- A^{-3}$ and minimum peaks of -0.37 and -0.82 $e^- A^{-3}$ in the vicinity of the metal atoms. Atomic scattering factors and associated anomalous dispersion factors were taken from the International Tables [8]. Final atomic coordinates, which are essentially identical for the two nitroprussides, and isotropic equivalent thermal parameters are presented in Table 3.

Results and Discussion

The crystallographic data pertaining to manganese and cadmium pentacyanonitrosylferrate trihydrate best fit a monoclinic lattice, space group $P2_1/n$ (No. 14, C_{2h}^5) with 4 molecules per unit cell. The lattice constants are $a = 7.302(4)$, $b = 14.783(6)$, $c = 10.751(1)$ Å and $\beta = 91.47(2)°$ for manganese nitroprusside and $a = 7.425(2)$, $b = 14.963(2)$, $c = 10.848(3)$ Å and $\beta = 91.64(2)°$ for cadmium nitroprusside. Five cyanide ligands and one nitrosyl group form a distorted octahedral arrangement about the iron atoms. Similarly, the metal atoms, Mn and Cd,

TABLE 3. Atomic coordinates ($\times 10^4$) and equivalent isotropic thermal parameters ($\times 10^3$) for (a) $Mn[Fe(CN)_5NO]\cdot 3H_2O$ and (b) $Cd[Fe(CN)_5NO]\cdot 3H_2O$

Atom	x	y	z	U_{eq} ($Å^2$)[a]
(a)				
Mn	7482.9(4)	3343.1(2)	3172.9(3)	16(3)
Fe	7527.4(4)	4214.9(2)	−2059.6(3)	13(2)
N(1)	4534(3)	617(1)	7705(2)	29(6)
N(2)	4634(3)	2712(1)	8122(2)	27(5)
N(3)	5425(3)	2241(1)	3572(2)	28(3)
N(4)	5326(3)	4409(1)	3032(2)	27(4)
N(5)	7773(3)	3640(1)	5193(2)	25(4)
C(1)	4401(3)	−83(1)	2539(2)	19(2)
C(2)	5688(3)	3275(1)	8059(2)	19(1)
C(3)	4367(3)	1693(1)	3339(2)	20(1)
C(4)	5710(3)	5060(1)	7304(2)	18(1)
C(5)	2714(3)	1154(1)	1214(2)	19(3)
N	2347(3)	411(1)	4387(2)	21(2)
O	2786(3)	5122(1)	9642(2)	47(24)
O(1)	1745(3)	1966(1)	6204(2)	34(8)
O(2)	2912(3)	3401(1)	915(2)	54(15)
O(3)	2599(3)	3680(2)	5376(3)	73(7)
(b)				
Cd	7386.3(3)	3339.4(2)	3178.9(2)	16(3)
Fe	7529.4(5)	4221.3(3)	−2035.2(5)	13(2)
N(1)	4559(4)	589(2)	7650(4)	33(7)
N(2)	4677(4)	2741(2)	8111(3)	29(6)
N(3)	5387(4)	2214(2)	3598(3)	30(4)
N(4)	5262(4)	4419(2)	3032(3)	27(4)
N(5)	7813(4)	3654(2)	5251(3)	29(5)
C(1)	4389(4)	−77(2)	2584(3)	20(1)
C(2)	5702(5)	3293(2)	8058(4)	22(2)
C(3)	4357(5)	1671(2)	3373(4)	19(2)
C(4)	5744(4)	5061(2)	7316(3)	19(1)
C(5)	2737(4)	1143(2)	1265(3)	20(2)
N	2315(4)	416(2)	4406(3)	22(3)
O	2843(4)	5138(2)	9639(3)	46(24)
O(1)	1646(5)	1980(2)	6137(3)	37(12)
O(2)	2881(4)	3397(2)	909(4)	58(13)
O(3)	2551(5)	3691(3)	5363(4)	83(13)

[a] U_{eq} is the isotropic equivalent thermal parameter and is defined as one-third the trace of the orthogonalized U_{ij} tensor.

are octahedrally coordinated by five cyanide ligands and one water molecule. The two metal centers are linked by cyanide bridging; M—N≡C—Fe is non-linear (see Fig. 1). The coordinated water molecules and bonded nitrosyl groups are geometrically arranged so that extensive tunnel-like formations permeate the crystal lattice. Unlike the hexacyanides, whose channels result from systematic $[Fe(CN)_6]^{3-}$ vacancies, the channels in the pentacyanides result from the replacement of a single bridged cyanide with a nitrosyl group and a coordinated water molecule. Such a replacement results in smaller, more selective pores, *c.* 5.23 × 5.29 Å for $Mn[Fe(CN)_5NO]$ and 5.32 × 5.37 Å for $Cd[Fe(CN)_5NO]$, when compared to those of the hexacyanide analogue Prussian blue, *c.* 5.6 × 8.6 Å [3]. The pore sizes were determined by calculating the Fe—C≡N—M distances which form the most restrictive parameters of the channels, see Fig. 2. The two uncoordinated water molecules are found within these channels hydrogen-bonded to the coordinated water molecule and possibly to the nitrosyl group.

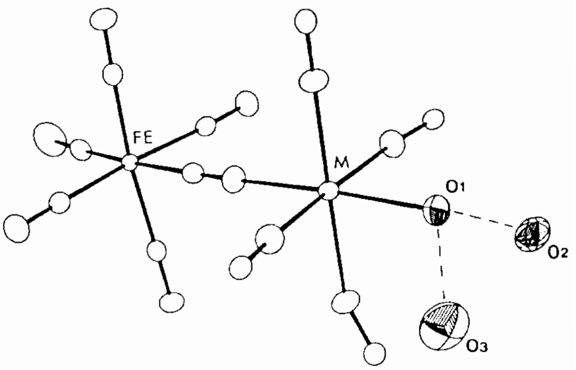

Fig. 1. A projected view of $M[Fe(CN)_5NO]\cdot 3H_2O$, where M = Mn or Cd, showing the distorted octahedral arrangements about the iron atoms, the cyanide bridging and the locations of the uncoordinated water molecules, O(2) and O(3), with respect to the coordinated water molecule, O(1).

For manganese nitroprusside, the averaged bond distances Mn—N (2.226 Å), Fe—C (1.935 Å) and C≡N (1.140 Å) as well as the bond distances of Mn—O(1) (2.218 Å), Fe—N (1.659 Å) and N=O (1.135 Å) are in good agreement with published values found in BIDICS [9]. The same is true for cadmium nitroprusside, where the averaged bond distances are Cd—N = 2.314, Fe—C = 1.942 and C≡N = 1.135 Å, and other notable bond lengths are Cd—O(1) = 2.335, Fe—N = 1.667 and N=O = 1.125 Å. There is strong directional bonding related to the interaction of Fe 3d orbitals and CN π orbitals as confirmed by the averaged Fe—C≡N bond angle of 177.9° for both compounds. The Fe—N length, being considerably shorter than the Fe—C length (see Table 4), most likely accounts for the distortion of the octahedral arrangement about the iron atoms. Also, it is evidenced by the reported bond angles in Table 5 that the greater electronegativity of the nitrosyl group with respect to the cyanide ligands causes deformation away from the nitrosyl end of the octahedral arrangement (N—Fe—C $> 90°$, C—Fe—C $< 90°$). An important aspect related to the electronegativity of groups ($NO > CN > H_2O$), which has been calculated by Huheey using the method of electronegativity equalization [10, 11], is the lowering of the charge coefficients which have the

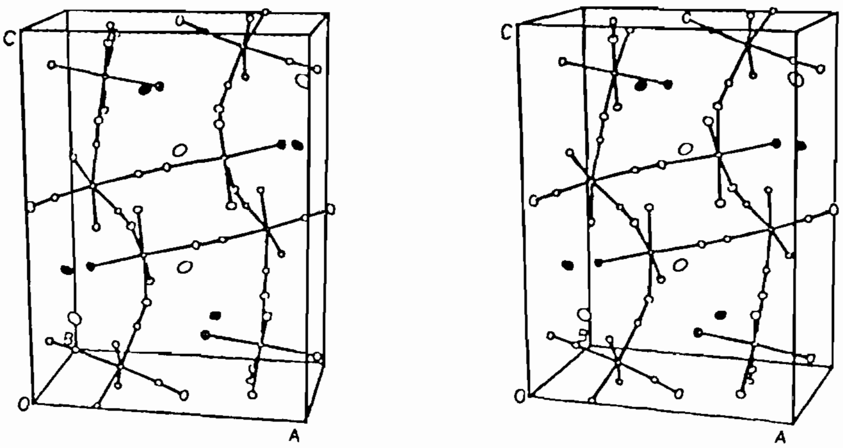

Fig. 2. A stereo view of M[Fe(CN)$_5$NO]·3H$_2$O, where M = Mn or Cd, revealing the extensive cyanide bridging and the positions of the uncoördinated water molecules, O(2) and O(3), within the channels. O(1) water molecules are represented by bonded, striated spheres; O(2) by solid spheres (●); and O(3) by hollow spheres (○).

TABLE 4. Bond and contact distances for (a) Mn[Fe(CN)$_5$NO]·3H$_2$O and (b) Cd[Fe(CN)$_5$NO]·3H$_2$O

Bond[a]	Distance (Å)	Bond	Distance (Å)
(a)			
Mn–N(1)	2.209(2)	Fe–C(1)	1.929(2)
Mn–N(2)	2.211(2)	Fe–C(2)	1.935(2)
Mn–N(3)	2.261(2)	Fe–C(3)	1.936(2)
Mn–N(4)	2.226(2)	Fe–C(4)	1.932(2)
Mn–N(5)	2.221(2)	Fe–C(5)	1.943(2)
Mn–O(1)	2.218(2)	Fe–N	1.659(2)
N(1)–C(1)	1.142(3)	N=O	1.135(2)
N(2)–C(2)	1.135(3)		
N(3)–C(3)	1.140(3)	O(1)–O(2)	2.854(3)
N(4)–C(4)	1.141(3)	O(1)–O(3)	2.759(3)
N(5)–C(5)	1.141(3)	O(2)–ON	2.886(3)
(b)			
Cd–N(1)	2.307(3)	Fe–C(1)	1.937(3)
Cd–N(2)	2.297(3)	Fe–C(2)	1.948(3)
Cd–N(3)	2.349(3)	Fe–C(3)	1.947(3)
Cd–N(4)	2.314(3)	Fe–C(4)	1.945(3)
Cd–N(5)	2.303(3)	Fe–C(5)	1.933(3)
Cd–O(1)	2.335(2)	Fe–N	1.667(3)
N(1)–C(1)	1.129(4)	N=O	1.125(3)
N(2)–C(2)	1.126(4)		
N(3)–C(3)	1.139(4)	O(1)–O(2)	2.856(4)
N(4)–C(4)	1.137(4)	O(1)–O(3)	2.784(4)
N(5)–C(5)	1.144(4)	O(2)–ON	2.949(4)

[a] O(1) = water molecule coordinated to the Mn or Cd atom. O(2) and O(3) = uncoordinated water molecules which lie within the channels.

effect of promoting charge transfer. The experimental results obtained in the study of the titled compounds strengthen the argument that orbital electronegativity and electronegativity equalization provide a useful

TABLE 5. Bond angles (°) for (a) Mn[Fe(CN)$_5$NO]·3H$_2$O and (b) Cd[Fe(CN)$_5$NO]·3H$_2$O

Atoms	Angle	Atoms	Angle
(a)			
N(1)–Mn–N(2)	89.97(7)	C(1)–Fe–C(2)	170.41(8)
N(1)–Mn–N(3)	177.27(7)	C(1)–Fe–C(3)	91.13(8)
N(1)–Mn–N(4)	88.51(8)	C(1)–Fe–C(4)	88.50(7)
N(1)–Mn–N(5)	92.13(7)	C(1)–Fe–C(5)	84.58(8)
N(1)–Mn–O(1)	94.28(7)	C(1)–Fe–N	93.57(8)
N(2)–Mn–N(3)	83.38(7)	C(2)–Fe–C(3)	88.05(9)
N(2)–Mn–N(4)	174.68(7)	C(2)–Fe–C(4)	90.96(8)
N(2)–Mn–N(5)	96.50(7)	C(2)–Fe–C(5)	85.84(8)
N(2)–Mn–O(1)	89.22(6)	C(2)–Fe–N	96.02(8)
N(3)–Mn–N(4)	92.93(7)	C(3)–Fe–C(4)	171.90(9)
N(3)–Mn–N(5)	90.22(6)	C(3)–Fe–C(5)	87.29(8)
N(3)–Mn–O(1)	83.52(6)	C(3)–Fe–N	95.36(8)
N(4)–Mn–N(5)	88.65(7)	C(4)–Fe–C(5)	84.62(8)
N(4)–Mn–O(1)	85.81(7)	C(4)–Fe–N	92.74(8)
N(5)–Mn–O(1)	171.41(6)	C(5)–Fe–N	176.80(7)
Mn–N(1)–C(1)	179.7(2)	Fe–C(1)–N(1)	177.8(2)
Mn–N(2)–C(2)	176.8(2)	Fe–C(2)–N(2)	178.6(2)
Mn–N(3)–C(3)	156.4(2)	Fe–C(3)–N(3)	178.7(2)
Mn–N(4)–C(4)	165.4(2)	Fe–C(4)–N(4)	176.6(2)
Mn–N(5)–C(5)	171.4(2)	Fe–C(5)–N(5)	178.0(2)
O(2)–O(1)–O(3)	111.5(1)	Fe–N–O	177.3(2)
(b)			
N(1)–Cd–N(2)	90.3(1)	C(1)–Fe–C(2)	170.2(1)
N(1)–Cd–N(3)	176.6(1)	C(1)–Fe–C(3)	90.4(1)
N(1)–Cd–N(4)	88.6(1)	C(1)–Fe–C(4)	88.7(1)
N(1)–Cd–N(5)	92.7(1)	C(1)–Fe–C(5)	84.7(1)
N(1)–Cd–O(1)	94.0(1)	C(1)–Fe–N	94.1(1)
N(2)–Cd–N(3)	88.5(1)	C(2)–Fe–C(3)	88.9(2)
N(2)–Cd–N(4)	174.2(1)	C(2)–Fe–C(4)	90.7(1)
N(2)–Cd–N(5)	96.8(1)	C(2)–Fe–C(5)	85.4(1)
N(2)–Cd–O(1)	89.8(1)	C(2)–Fe–N	95.8(1)

(continued)

TABLE 5. *(continued)*

Atoms	Angle	Atoms	Angle
N(3)–Cd–N(4)	92.2(1)	C(3)–Fe–C(4)	171.9(1)
N(3)–Cd–N(5)	90.6(1)	C(3)–Fe–C(5)	87.1(1)
N(3)–Cd–O(1)	82.8(1)	C(3)–Fe–N	95.4(1)
N(4)–Cd–N(5)	88.9(1)	C(4)–Fe–C(5)	84.8(1)
N(4)–Cd–O(1)	84.6(1)	C(4)–Fe–N	92.7(1)
N(5)–Cd–O(1)	170.5(1)	C(5)–Fe–N	177.2(1)
Cd–N(1)–C(1)	177.8(3)	Fe–C(1)–N(1)	178.3(3)
Cd–N(2)–C(2)	177.3(3)	Fe–C(2)–N(2)	178.4(3)
Cd–N(3)–C(3)	156.5(3)	Fe–C(3)–N(3)	177.7(3)
Cd–N(4)–C(4)	164.4(3)	Fe–C(4)–N(4)	176.9(3)
Cd–N(5)–C(5)	170.4(3)	Fe–C(5)–N(5)	178.0(3)
O(2)–O(1)–O(3)	113.6(1)	Fe–N–O	177.3(3)

avenue to the question of charge distribution in molecules. The coordinated water molecule, O(1), bonded to the metal atom, Mn or Cd, is less electronegative in character than the cyanide ligands, causing deformation of the distorted octahedral array towards the coordinated water molecule. However, an anomaly is observed related to the N(1)–M–O(1) angle in each system. The angle should be less than 90° instead of 94°. This is accounted for by the distortion of the N(5)–M–O(1) angle from ideality, 180° (see Table 5). Despite the anomaly, the deformation is still towards the coordinated water molecule. This alternating deformation about the iron and metal centers is responsible for the serpentine appearance of the crystal lattice (see Fig. 2).

Important intermoiety oxygen–oxygen contact distances for manganese and cadmium nitroprussides are listed in Table 4. The differences in contact lengths O(1)···O(2) and O(1)···O(3) are significant in each studied system, 2.854(3) and 2.759(3) Å for $Mn[Fe(CN)_5NO]\cdot 3H_2O$ and 2.856(4) and 2.784(4) Å for $Mn[Fe(CN)_5NO]\cdot 3H_2O$. The respective contact lengths for O(2)···ON are 2.886(3) and 2.949(4) Å. Studies by Brown [12] on the geometry of hydrogen bonds have demonstrated that O···O intermolecular distances of approximately 2.73 Å or less are considered to be strong hydrogen bonds (assuming no geometric constraints) and that hydrogen bonds become progressively weaker as the contact distance increases. The difference in contact distances of O(1)···O(3) and O(1)···O(2) as well as for O(2)···ON suggest that two different types of hydrogen bonding are present in the titled compounds, strong and weak hydrogen bonds. This difference in the intermolecular O···O distances, being related to hydrogen bonds, is further evidenced by the hydrogen bonding doublet bands observed in the IR spectra (see Table 2). Similar conclusions have been published related to the crystal structure of $In(OH)_3$ by X-ray and neutron diffraction methods [13, 14]. Further, based on the observed oxygen–oxygen distances and the O(2)–O(1)–O(3) bond angle, 111.2° for $Mn[Fe(CN)_5NO]\cdot 3H_2O$ and 113.6° for $Cd[Fe(CN)_5NO]\cdot 3H_2O$, it would appear that the hydrogen atoms on the coordinated O(1) water molecules are responsible for the positioning of the uncoordinated water molecules within the channels, an ideal H–O–H angle = 104.5°. For Prussian blue, $Fe_4[Fe(CN)_6]_3\cdot xH_2O$, hydrogen bonding through the hydrogen atoms of the coordinated water molecule, this is O(1) in our studies, has been confirmed by neutron diffraction studies of Herren *et al.* [15]. Neutron diffraction studies of Prussian blue have also confirmed two crystallographically and chemically distinct kinds of water molecules within its framework. This also appears to be the case with the nitrosyl analogues (the titled compounds). Neutron diffraction studies on these zeolitic type compounds should clarify any questions pertaining to the orientations of the hydrogen atoms and give insight into the semipermeable membrane properties of the nitroprussides.

Supplementary Material

Full listings of anisotropic thermal parameters and observed and calculated structure factors are available from author D.F.M.

Acknowledgement

The authors wish to acknowledge the financial support of The Robert A. Welch Foundation (Grant No. AA-668).

References

1 E. Kalecinska and B. Jesowska-Trzebiatowska, *Radiochem. Radioanal. Lett., 44* (1980) 17.

2 J. Narbutt, J. Siwinski, B. Bartos and A. Bilewicz, *J. Radioanal. Nucl. Chem., 101* (1986) 41.

3 G. Boxhoorn, J. Moolhuysen, J. F. C. Coolegem and R. A. van Santen, *J. Chem. Soc., Chem. Commun.,* (1985) 1305.

4 D. F. Mullica, E. L. Sappenfield, D. B. Tippin and D. Leschnitzer, *Inorg. Chim. Acta, 164* (1989) 99.

5 A. Ludi, H. U. Gudel and M. Ruegg, *Inorg. Chem., 9* (1970) 2224.

6 H. J. Buser, D. Schwarzenbach, W. Petter and A. Ludi, *Inorg. Chem., 16* (1977) 2704.

7 Enraf-Nonius, *VAX Structure Determination Package,* Delft, The Netherlands, 1985.

8 J. A. Ibers and W. C. Hamilton, *International Tables for X-ray Crystallography,* Vol. IV, Kynoch Press, Birmingham, U.K., 1974.

9 *BIDICS, Bond Index of the Determination of Inorganic Crystal Structures,* Institute for Materials Research, Hamilton, Canada, 1969–1981.

10 J. E. Huheey, *J. Phys. Chem., 69* (1965) 3284.

11 J. E. Huheey, *J. Phys. Chem., 70* (1966) 2086.
12 I. D. Brown, *Acta Crystallogr., Sect. A, 32* (1976) 24.
13 A. N. Christensen, R. Gronbaek and S. F. Rasmussen, *Acta Chem. Scand., 18* (1964) 1261.
14 D. F. Mullica, G. W. Beall, W. O. Milligan, J. D. Korp and I. Bernal, *J. Inorg. Nucl. Chem., 41* (1979) 277.
15 F. Herren, P. Fischer, A. Ludi and W. Halg, *Inorg. Chem., 19* (1980) 956.